Dynamic and Static Light Scattering by Aqueous Polyacrylamide Gels

Jacques G. H. Joosten* and Jennifer L. McCartney

Department for Physical & Analytical Chemistry, DSM Research, P.O. Box 18, 6160 MD Geleen, The Netherlands

Peter N. Pusey

Physics Department, University of Edinburgh, Mayfield Road, EH9 3JZ Edinburgh, United Kingdom

Received May 7, 1991; Revised Manuscript Received July 31, 1991

ABSTRACT: Dynamic light scattering (DLS) and static light scattering (SLS) experiments on cross-linked polyacrylamide (PAA) gels show that these systems exhibit nonergodic behavior; i.e., the time-averaged intensity correlation function (ICF), the quantity obtained from a single DLS experiment, is not equal to the ensemble-averaged ICF. Treating the gels as arbitrary nonergodic media, the intermediate scattering function (ISF) is extracted from single DLS experiments. The initial decay of the ISF yields a diffusion coefficient that takes into account all density fluctuations. Particularly, at high cross-link density or high total monomer content the ISF's show a nondecaying component resulting from frozen-in density fluctuations. The ensemble-averaged scattered intensity shows a clear angular dependence, implying long-range (≈500-nm) correlation lengths in the gels. By combining DLS and SLS the fluctuating part of the scattered light can be separated from the total scattered intensity. This fluctuating component is hardly angle dependent and surprisingly appears to be somewhat larger for gels than for polymer solutions at the same concentrations, implying smaller osmotic moduli for gels than for solutions. Furthermore, the analysis shows that the mobility of the polymer is larger in gels than in analogous solutions.

I. Introduction

In this paper we describe and discuss experiments by dynamic light scattering (DLS) and static light scattering (SLS) on gels produced by copolymerizing acrylamide and bisacrylamide. Aqueous polyacrylamide (PAA) gels are used in a large number of applications in science and technology.[1] These polymeric gels have been studied extensively by light, X-ray, and neutron scattering with the aim of identifying their microscopic (network) structure and dynamics.[2-13] Here we emphasize two aspects: the nonergodicity of the gel medium which arises from the presence of permanent cross-links between the polymer coils, and complications associated with "(micro)inhomogeneities" having spatial scales, on the order of several hundreds of nanometers, much larger than the average distance between cross-links, which is typically ≈5 nm.[14]

An ideal (theorist's) gel can be viewed as a three-dimensional random collection of polymer coils having their ends connected to cross-links, the functionality of the cross-links being constant throughout the sample. On a (semi)microscopic scale such a gel is structurally similar to the equivalent (semidilute) solution, showing only short-ranged correlations. However, with respect to the dynamics on this scale, it is different. In a solution, the polymer molecules are able to diffuse throughout the sample so that, given enough time, the system evolves through a sequence of spatial configurations representative of the full ensemble of possible configurations (or, equivalently, of the whole of phase space). By contrast, in a gel, the polymer segments are restricted by the cross-links to particular regions of the sample and are only able to perform limited Brownian motions about fixed average positions. As a result, one particular sample of a gel is trapped in a restricted region of phase space defined by its average configuration and the extent of the fluctuations about this configuration. A gel may thus be regarded as a nonergodic medium since a time-averaged measurement on a particular sample will not, in general, be equivalent to an ensemble-averaged measurement; i.e., one averaged over a representative number of all possible spatial configurations. de Gennes[14] has put forward the idea of a gel being very much like a glass; what he calls the "final ensemble" is a frozen state that can behave differently from a usual equilibrium system.

Recent experiments on colloidal glasses[15,16] and tracer particles trapped in PAA gels[17] have shown that, in agreement with earlier theoretical work,[18] nonergodicity of the medium can have profound effects on dynamic light scattering measurements. DLS measures the time-averaged time correlation function of the intensity $I(q,t)$ of light scattered by the sample in the direction described by the scattering vector $\mathbf{q}$, $|\mathbf{q}| = (4\pi/\lambda)\sin(\theta/2)$, λ and θ being the wavelength of the light and the scattering angle in the medium, respectively. This intensity is proportional to $|\rho(q,t)|^2$ where $\rho(q,t)$ is the qth spatial Fourier component of the fluctuations causing the scattering. In the case of polymer systems, these are fluctuations in the concentration of polymer segments. For a nonergodic medium $\rho(q,t)$ comprises a nonfluctuating, or constant, component, associated with the fixed average configuration of the sample, and a fluctuating component, associated with the restricted Brownian motions of the polymer segments. The complications in DLS by nonergodic media arise from the constant component of $\rho(q,t)$, which is zero for an ergodic medium.

As mentioned above, from a structural point of view an ideal gel is similar to the equivalent solution. Thus, the (ensemble-)averaged intensities of radiation scattered by each system should be much the same. In fact, it is frequently found that real gels such as polyacrylamide scatter much more strongly than solutions at the same concentration.[7,8] Furthermore, the intensity of scattered light can show a significant dependence on scattering vector q. These observations indicate the presence of concentration fluctuations or inhomogeneities in the gel which have spatial extent or correlation range comparable to the

0024-9297/91/2224-6690$02.50/0

wavelength of light, i.e., several hundred nanometers. The origin and properties of these inhomogeneities have been discussed by Dusek and Prins[19] and by Bastide and Leibler.[20]

Here we take two approaches to interpreting the dynamic light scattering by polyacrylamide gels containing inhomogeneities. First we consider them as arbitrary nonergodic media and apply the analysis of refs 17 and 18 to obtain ensemble-averaged intermediate scattering functions $f(q,\tau) = \langle \rho(q,0)\ \rho^*(q,\tau)\rangle_E / \langle |\rho(q,0)|^2\rangle_E$, where the subscript E denotes an ensemble average. From these intermediate scattering functions we obtain the diffusion coefficients describing their initial decays and their nondecaying components $f(q,\infty)$. From $f(q,\infty)$ we can further calculate the (ensemble-) averaged intensities of the fluctuating and constant components of $\rho(q,t)$. An interesting finding is that the magnitudes of the fluctuating components in the gels are similar to those in the equivalent solutions.

This finding supports a second treatment: In this approach the large-scale inhomogeneities are regarded as "uninteresting" features which provide a static scattering which mixes or heterodynes with the "interesting" fluctuating scattering. In fact this approach has been used previously by many workers[10,21] in the field of gels, where the diffusion coefficient associated with the fluctuating component of the scattered light is interpreted in terms of a viscoelastic model of the gel.[2]

The paper is organized as follows: in section II the relevant notions and equations for interpreting the light scattering data are given. Section III includes the experimental details and a results and discussion section which are presented for two sets of PAA samples: one set in which the total monomer content of the gels is kept constant (at 2.5 wt %) whereas the cross-link content is varied and the other set where the total monomer content is varied at a constant ratio bisacrylamide/acrylamide. In section IV we given some concluding remarks concerning the experimental findings.

II. Theoretical Background

This section is intended only as a survey of the expressions directly pertinent to the discussion of DLS on gels. For a rigorous treatment and a thorough theoretical discussion of DLS experiments on nonergodic media, see the paper by Pusey and van Megen.[18]

The amplitude $E(q,t)$ of the electric field of light scattered by a medium undergoing fluctuations $\rho(r,t)$ in density (or refractive index) can be written

$$E(q,t) \sim \rho(q,t) = \int_v d^3\mathbf{r}\ \rho(\mathbf{r},t)\ \exp[i\mathbf{q}\cdot\mathbf{r}] \qquad (1)$$

For both methods of data analysis to be used in this paper the scattered field at the detector can be written as the sum of two components

$$E(q,t) = E_F(q,t) + E_C(q) \qquad (2)$$

where the fluctuating component $E_F(q,t)$ is a zero-mean complex Gaussian variable and $E_C(q)$ is a constant (time-independent) field. When the gel is regarded as an arbitrary nonergodic medium, the constant field is that arising from the "frozen-in" density fluctuations.[18] For the heterodyne case, $E_C(q)$ is simply the field scattered by the "uninteresting" large-scale inhomogeneities, which provides the local oscillator.

A single DLS measurement provides an estimate of $g_T^{(2)}(q,\tau)$, the time-averaged normalized time correlation function of the scattered intensity

$$g_T^{(2)}(q,\tau) \equiv \frac{\langle I(q,0)\ I(q,\tau)\rangle_T}{\langle I(q,0)\rangle_T^2} \qquad (3)$$

where the intensity is given by $I(q,t) = |E(q,t)|^2$, τ denotes time, and $\langle ...\rangle_T$ indicates a time average. For a field of the form of eq 2 it is straightforward to show that (see, e.g., ref 22)

$$g_T^{(2)}(q,\tau) - 1 = \frac{\langle E_F(q,0)E_F^*(q,\tau)\rangle_T^2 + 2I_C(q)\langle E_F(q,0)E_F^*(q,\tau)\rangle_T}{\langle I(q,0)\rangle_T^2} \qquad (4)$$

where

$$\langle I(q)\rangle_T = \langle I_F(q)\rangle_T + I_C(q) \qquad (5)$$

with $I_F(q,t) = |E_F(q,t)|^2$ and $I_C(q) = |E_C(q)|^2$.

Equation 4 can now be evaluated for the two situations under consideration, i.e., the nonergodic and the heterodyne approach.

For an arbitrary nonergodic medium it has been shown elsewhere[18] that

$$\langle E_F(q,0)\ E_F^*(q,\tau)\rangle_T = \langle E_F(q,0)\ E_F^*(q,\tau)\rangle_E = \langle I(q)\rangle_E[f(q,\tau) - f(q,\infty)] \qquad (6)$$

where $\langle ...\rangle_E$ indicates an ensemble average over all possible configurations of the medium and the normalized intermediate scattering function $f(q,\tau)$ is given by

$$f(q,\tau) = \frac{\langle \rho(q,0)\ \rho^*(q,\tau)\rangle_E}{\langle |\rho(q)|^2\rangle_E} \qquad (7)$$

The zero-time limit of eq 6 gives

$$\langle I_F(q)\rangle_T = \langle I(q)\rangle_E[1 - f(q,\infty)] \qquad (8)$$

Equation 4 can be solved[17] for the intermediate scattering function, with use of eqs 5, 6, and 8, giving

$$f(q,\tau) = 1 + \frac{1}{Y}[\sqrt{g_T^{(2)}(q,\tau) - \sigma_I^2} - 1] \qquad (9)$$

where the mean-square intensity fluctuation σ_I^2 is given by

$$\sigma_I^2 \equiv \frac{\langle I^2(q)\rangle_T}{\langle I(q)\rangle_T^2} - 1 = g_T^{(2)}(q,0) - 1 \qquad (10)$$

and

$$Y \equiv \frac{\langle I(q)\rangle_E}{\langle I(q)\rangle_T} \qquad (11)$$

A short-time expansion of $f(q,\tau)$ reads

$$f(q,\tau) = 1 - D(q)\ q^2\tau + ... \qquad (12)$$

where $D(q)$ is the diffusion coefficient describing the initial decay of the density correlations $\langle \rho(q,0)\ \rho^*(q,\tau)\rangle_E$ and therefore takes into account all the processes contributing to the light scattering. As discussed in ref 18, one can also define an apparent diffusion coefficient by

$$D_A(q) = -\frac{1}{q^2}\lim_{\tau\to 0}\frac{\partial \ln}{\partial \tau}[\sqrt{g^{(2)}(q,\tau) - 1}] \qquad (13)$$

This is the quantity which would be obtained if the light scattering from a nonergodic medium were (incorrectly) analyzed as if the medium were ergodic. It can be shown[18]

that the two diffusion coefficients are related by

$$D(q) = \frac{D_A(q)\,\sigma_I^2}{Y} \tag{14}$$

In the heterodyne approach one separates the light scattering from gels into contributions from concentration fluctuations of the network and contributions from (static) macroscopic inhomogeneities. Only the former are assumed to be relevant whereas the latter contributions provide the local oscillators for optical heterodyne detection.[9,21,23]

For the heterodyne case we define an intermediate scattering function $f_N(q,\tau)$, associated with the relevant dynamic component of the density fluctuations of the network by

$$f_N(q,\tau) = \frac{\langle E_F(q,0)\,E_F^*(q,\tau)\rangle_T}{\langle I_F(q)\rangle_T} \tag{15}$$

Solving now eq 4 by using eqs 5 and 15 gives

$$f_N(q,\tau) = 1 + \frac{1}{X}[\sqrt{g_T^{(2)}(q,\tau) - \sigma_I^2} - 1] \tag{16}$$

where

$$X \equiv \frac{\langle I_F(q)\rangle_T}{\langle I(q)\rangle_T} \tag{17}$$

The ratio X can be found from the infinite-time limit of eq 16

$$X = 1 - \sqrt{1 - \sigma_I^2} \tag{18}$$

We can further define the diffusion coefficient $D_N(q)$ associated with $f_N(q,\tau)$ by

$$f_N(q,\tau) = 1 - D_N(q)\,q^2\tau + \ldots \tag{19}$$

In order to relate $D(q)$ and $D_N(q)$, we rewrite eq 4 for the heterodyne case leading to

$$g_T^{(2)}(q,\tau) - 1 = X^2 f_N^2(q,\tau) + 2X(1-X)f_N(q,\tau) \tag{20}$$

where eqs 15 and 17 have been used.[24]

Substituting eq 20 and $\sigma_I^2 = X(2-X)$ from eq 18 into eq 9 and using the short-time expansions of $f(q,\tau)$ and $f_N(q,\tau)$ show that the diffusion coefficients $D(q)$ and $D_N(q)$ are related by (see also eq 25)

$$D_N(q) = \frac{YD(q)}{X} = \frac{D(q)}{1 - f(q,\infty)} \tag{21}$$

We will now briefly discuss a few general features of the results obtained so far.

Although there exists a formal similarity between eqs 9 and 16, which provide the intermediate scattering functions $f(q,\tau)$ and $f_N(q,\tau)$ from experimental data for $g_T^{(2)}(q,\tau)$, one is faced with a fundamental difference: in the heterodyne approach one *assumes* that the inhomogeneities do not constitute a relevant part of the gel system whereas in treating the gel as a general nonergodic medium one inherently takes into account all the features of the gel without making any assumptions as to what is relevant or irrelevant. From reported experimental studies on various gels it seems that inhomogeneities are intrinsic objects in such systems.[19,20,25,26] It is also known that these "imperfections" in the network structure strongly influence the properties of gels such as the solvent permeability, the diffusion of molecules (electrophoresis), and the elastic properties.[19,25,27] Furthermore, Hecht et al.[7] have shown by scattering experiments that structural inhomogeneities in PAA gels may have dimensions in the range 1 nm to 0.25 μm, implying that the notion "large scale" is rather ambiguous. Thus it appears that the so-called large-scale inhomogeneities should be dealt with, both theoretically and experimentally. Nevertheless, in this paper we will interpret the experimental data by using the heterodyne approach as well as treating the gels as general nonergodic media.

III. Experimental Section

A. Materials and Sample Preparation. Ultragrade-quality acrylamide (AA), *N,N'*-methylenebisacrylamide (BAA), ammonium persulfate, and *N',N'*-tetramethylethylenediamine (TEMED) were used as purchased from LBK-Produkter AB, Sweden. Water was obtained from a Milli-Q reagent-grade system (Millipore) and was thrice filtered through 0.05-μm paper.

Stock solutions were made by mixing appropriate amounts of acrylamide and bisacrylamide followed by 30 min of ultrasonication. The final, total monomer content [AA] + [BAA], expressed as C_T (g/100 g), was varied from 2 to 10% at a constant cross-link density ([BAA]/[AA]), expressed as a weight fraction C (%), of 1%. The cross-link content C was also varied from 0 to 4% at a constant C_T of 2.5%.

Polymerization was carried out by mixing stock solution, water, and 1 μL of TEMED in a clean cylindrical optical glass cuvette (diameter = 1 cm) up to a total volume of 2 mL. With the addition of 15 μL of initiator (ammonium persulfate, 10 wt % solution), the solutions were flushed with N_2 for 30 s. Polymerization is thought to be completed within 30 min at room temperature, but no measurements were done within the first 24 h. All the samples were macroscopically homogeneous and optically clear.

B. Experimental Setup and Methods. Light scattering measurements were accomplished by using the apparatus and methods described in ref 17. In summary the instrument comprises an ALV/SP-86 goniometer (ALV, Langen, Germany) equipped with an Ar^+ laser operating at an output power of ≈450 mW. The incident beam (wavelength in vacuo, λ_0 = 514.5 nm) is polarized vertically with respect to the scattering plane. A Glan-Thomson prism is used for detecting only vertically polarized scattered light. Intensity correlation functions (ICF's) are measured by an ALV-3000 multibit correlator (ALV, Langen, Germany). For the experiments described here, the correlator was operated in the so-called multi-τ mode, yielding a $g_T^{(2)}(q,\tau)$ that consists of 192 logarithmically spaced channels allowing a time span of 9 decades in one run. Normalization of the ICF's is accomplished by using the total number of photon counts and the number of summations from the correlator, thereby using the built-in option of symmetrical normalization.[28] ICF data to be used for the analysis were obtained by taking the average of the results of 10 runs each of 3–5-min duration.

As will be described in section III.C, the scattered intensity $\langle I(q)\rangle_T$, at a particular scattering angle, varies strongly when scanning through various positions in the sample (see Figure 1). Therefore, methods were developed that enable an estimation of $\langle I(q)\rangle_E$ and a determination of the properties of $\langle I(q)\rangle_T$.

The procedure for determining the ensemble-averaged intensity, $\langle I(q)\rangle_E$, is described in ref 17. There a manual method was followed. Here we used an automated procedure by having a stepping motor attached to the sample cuvette. This motor is interfaced to and driven by the same computer that controls the correlator. To obtain $\langle I(q)\rangle_E$, the count rate was the only data read from the correlator. The count rate was measured for 15 s during which the cylindrical sample cell was continuously rotated by the stepping motor at a speed of 30 rpm. This measurement was repeated 10 times at each scattering angle, and $\langle I(q)\rangle_E$ is taken as the average count rate. Although relative intensities were obtained accurately, we did not measure absolute scattering cross sections.

The properties of $\langle I(q)\rangle_T$ are studied by measuring the probability distribution $P(\langle I(q)\rangle_T)$. In this experiment the count rate for a particular scattering volume or "speckle" was recorded using an integration time of 15 s; then the sample was rotated a random number of steps and stopped, and the count rate was

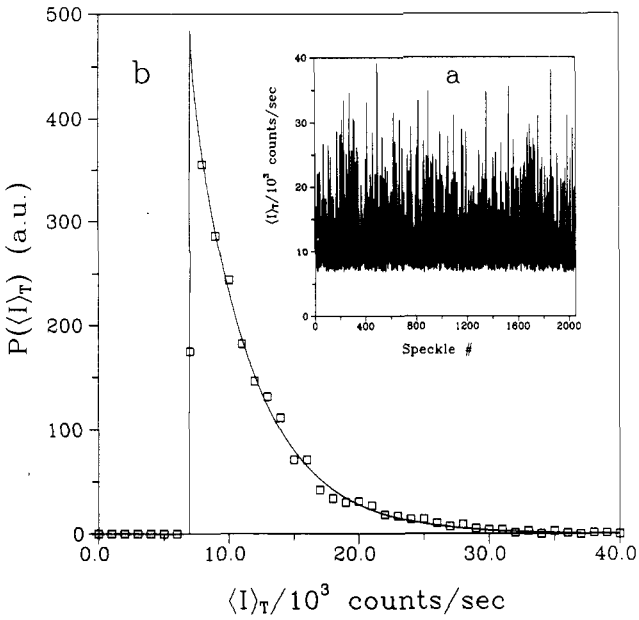

Figure 1. (a) $\langle I(q)\rangle_T$ for various speckles as obtained by scanning through various positions in the sample. Data are taken from a gel with $C_T = 2.5\%$ and $C = 1.6\%$ at a scattering angle $\theta = 150°$. (b) Frequency distribution, $P(\langle I(q)\rangle_T)$, of the data given in a. Solid line: least-squares fit of eq 23 to the data resulting in $\langle I_F(q)\rangle_T = \langle I_F(q)\rangle_E = 7 \times 10^3$ counts/s and $\langle I(q)\rangle_E = 11.7 \times 10^3$ counts/s.

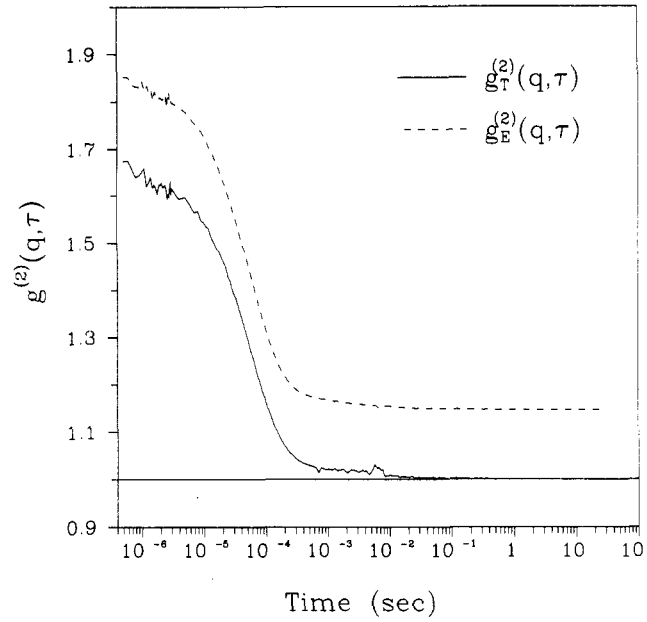

Figure 2. Ensemble-averaged intensity correlation function $g_E^{(2)}(q,\tau)$ (– –) and time-averaged intensity correlation function $g_T^{(2)}(q,\tau)$ (—) obtained at a scattering angle $\theta = 90°$ on the same sample ($C_T = 2.5\%$, $C = 1.6\%$).

again measured. This whole process was repeated up to 1000–2000 times for a given sample and scattering angle.

The stepping motor used in conjunction with the correlator allows ensemble-averaged correlation functions, $g_E^{(2)}(q,\tau)$, to be collected in a semiautomated fashion. Estimates for $g_E^{(2)}(q,\tau)$ were obtained with the correlator also set to multi-τ mode. In these measurements the stepping motor turns a random number of steps and then stops, and the correlator starts collecting data for a certain period (typically, 5–10 min). When the correlator is finished, the motor again turns a random number of steps and the correlator is restarted without clearing the memory. This procedure is repeated a large number of times (typically, 50–100), the data being accumulated in the 192 channels. Then the total correlation function data are read from the correlator and normalized by the total number of photon counts and the number of summations. From this ensemble-averaged intensity correlation function an intermediate scattering function was calculated by using the well-known (Siegert) relation

$$g_E^{(2)}(q,\tau) = 1 + |\beta f(q,\tau)|^2 \tag{22}$$

where β is the spatial coherence factor which depends largely on the number of coherence areas seen by the detector.[22,29] For our experimental setup β was determined to be 0.94 ± 0.02 using a standard polystyrene latex dispersion.[17]

C. Results and Discussion. Time-averaged intensity distribution: The nonergodic nature of the gel systems is immediately apparent from the following observations: Using the method described in section III.B for scanning through various positions in the sample, a large variation in time-averaged scattered intensity $\langle I(q)\rangle_T$ is revealed. A typical result is shown in Figure 1a for a sample with $C_T = 2.5\%$ and $C = 1.6\%$ at a scattering angle $\theta = 150°$. This observation implies that we are observing different subensembles of the total configuration space. It is found that $\langle I(q)\rangle_T$ for a particular position (speckle, scattering volume) and fixed scattering angle remains constant for a long time, i.e., minutes for weak gels (low cross-linking) and hours for strong gels (high cross-linking). In general, un-cross-linked gels do not show this feature; i.e., $\langle I(q)\rangle_T$ is the same for all scattering volumes and is equal to $\langle I(q)\rangle_E$. From the data depicted in Figure 1a a histogram is constructed by grouping the data in intervals of 1 kcounts/s, resulting in an estimate of the probability distribution function $P(\langle I(q)\rangle_T)$ of the scattered intensity, $\langle I(q)\rangle_T$, sampled over the full ensemble. The result of $P(\langle I(q)\rangle_T)$ vs $\langle I(q)\rangle_T$ is shown in Figure 1b. The probability distribution function shows a cutoff at low intensities resulting from the contribution $\langle I_F(q)\rangle_T$, the average of the fluctuating component $I_F(q,t)$. In addition to this we expect a negative exponential part resulting from $I_C(q)$ (see eq 5). It is shown that[17]

$$P(\langle I(q)\rangle_T) \sim H(\langle I(q)\rangle_T - \langle I_F(q)\rangle_T) \exp\left[-\frac{\langle I(q)\rangle_T - \langle I_F(q)\rangle_T}{\langle I(q)\rangle_E - \langle I_F(q)\rangle_T}\right] \tag{23}$$

where $H(x)$ is the Heaviside function, $H(x) = 0$ for $x < 0$ and $H(x) = 1$ for $x > 0$.

In deriving eq 23 it is assumed that the integration time for measuring $\langle I(q)\rangle_T$ is chosen such that it comprises many typical decay times of the fast fluctuations in the system. The solid line in Figure 1b is a nonlinear least-squares fit of the function given in eq 23 to the data. One notices that the data are well described by this function which implies that the scattered field $E(q,\tau)$, associated with this intensity, is a zero-mean Gaussian stochastic variable when sampled over the full ensemble. From the parameters used to construct the curve in Figure 1b we find $\langle I_F(q)\rangle_T = 7$ kcounts/s and $\langle I(q)\rangle_E = 11.7$ kcounts/s; the procedure, described in section III.B, for obtaining $\langle I(q)\rangle_E$ also gives 11.7 kcounts/s. By using eq 8 we find $f(q,\infty) = 0.40$ from these data. This value agrees very well with the result we obtain for $f(q,\infty)$ from the analysis of time-averaged ICF's to be described below.

Geissler et al.[6] and Mackie et al.[31] also observed a variation of the scattered intensity when scanning through gel samples, but these authors did not present an analysis of their results. Kobayasi[32] seems to have been the first to propose a method for measuring $\langle I(q)\rangle_T$ at various positions in gel systems. His approach and its relation to eq 23 is discussed in ref 17.

DLS experiments: An ensemble-averaged ICF, $g_E^{(2)}(q,\tau)$ (requiring a collection time of approximately 8 h), and a time-averaged ICF, $g_T^{(2)}(q,\tau)$ (requiring a measuring time of 30 min), are compared in Figure 2 for a sample with $C_T = 2.5\%$ and $C = 1.6\%$ at a scattering angle $\theta = 90°$. The ensemble-averaged ICF was constructed following the procedure described in section III.B from unnormalized ICF's of 100 different speckles. From Figure 2 the nonequivalence of the time- and ensemble-averaged ICF's is obvious. The results show the behavior expected for a nonergodic medium, and it would be clearly incorrect to simply read the time-averaged ICF from the correlator and assume it to be equivalent with the ensemble-averaged ICF. From the ensemble-averaged data shown in Figure 2 the spatial coherence

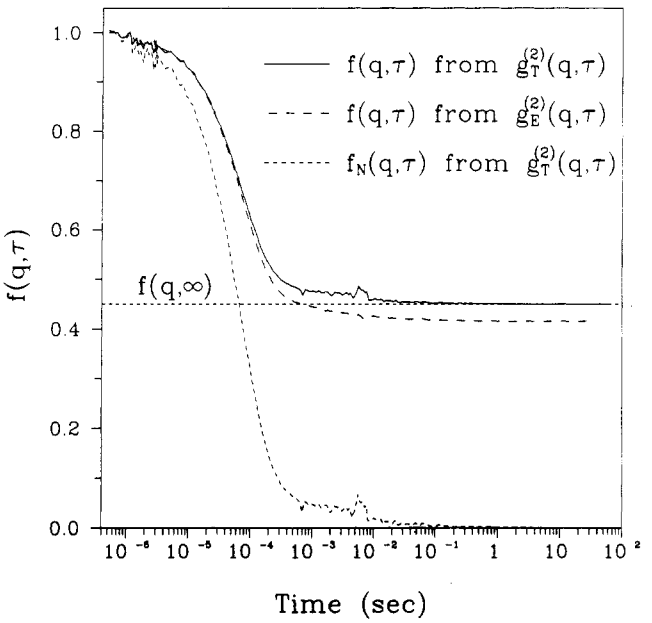

Figure 3. Intermediate scattering functions, $f(q,\tau)$, calculated from the results given in Figure 2: (– –) $f(q,\tau)$ obtained from $g_E^{(2)}(q,\tau)$ using eq 22; (—) $f(q,\tau)$ obtained from $g_T^{(2)}(q,\tau)$ using eq 9; (- - -) $f_N(q,\tau)$ obtained from $g_T^{(2)}(q,\tau)$ using eq 16. Normalization of the $f(q,\tau)$'s at $\tau = 0$ is described in the text. $f(q,\infty)$ Is the fraction of frozen-in fluctuations found from $g_T^{(2)}(q,\tau)$.

Table I
Frozen-In Component $f(q,\infty)$ for the Sample with $C_T = 2.5\%$ and $C = 1.6\%$ As Obtained from Three Different Methods

θ	$f(q,\infty)^a$	$f(q,\infty)^b$	$f(q,\infty)^c$
30	0.61	0.68	
90	0.42	0.45	0.42
150	0.40	0.42	

[a] From time-averaged intensity distribution $P(\langle I(q)\rangle_T)$. [b] From $f(g,\tau)$ as calculated from $g_T^{(2)}(q,\tau)$. [c] From $f(q,\tau)$ as found from $g_E^{(2)}(q,\tau)$.

factor β can be calculated to be 0.92. In the limit where an infinite number of speckles is used to construct the ensemble average, β should be equal to the value 0.94 as measured for an ergodic system (see section III.B). The small difference is most likely explained as a result of the finite number of measurements, in this case 100.

Although the time- and ensemble-averaged ICF's will be different for a nonergodic medium, the intermediate scattering functions, $f(q,\tau)$, obtained from the two ICFs should be equivalent. Obviously, $f(q,\tau)$ can be calculated from $g_E^{(2)}(q,\tau)$ by using eq 22. The result is shown in Figure 3 where normalization at $\tau = 0$ is accomplished by using $\beta = 0.92$. To obtain $f(q,\tau)$ from $g_T^{(2)}(q,\tau)$, we used eq 9, and the result is also given in Figure 3. Although eq 9 ensures that $f(q,0) = 1$, one has to take into account the fact that the size of the detector aperture is not negligible compared to the size of a speckle; i.e., the detector performs some spatial integration, $\beta < 1$. We performed an aperture correction by using the analysis described in ref 29.

As can be seen from Figure 3 the agreement between the two $f(q,\tau)$'s is reasonably good. The slight difference, particularly at long times, can be explained by any of the following: too few subensembles for ensemble construction, small variations in the setup during the collection time of $g_E^{(2)}(q,\tau)$ (8 h), and uncertainties with respect to β.[33]

Referring to Figures 1 and 3, $f(q,\infty)$ can be obtained from either $P(\langle I(q)\rangle_T)$ or $f(q,\tau)$. Since $f(q,\infty)$ is a characteristic property of the sample (a measure of the frozen-in density fluctuations), it should be independent of the method of data analysis. In Table I we compare the results for $f(q,\infty)$ as obtained by three different methods on the sample with $C_T = 2.5\%$ and $C = 1.6\%$ at scattering angles $\theta = 30°$, 90°, and 150°. The values agree quite well within experimental errors, which shows the consistency of the various methods.

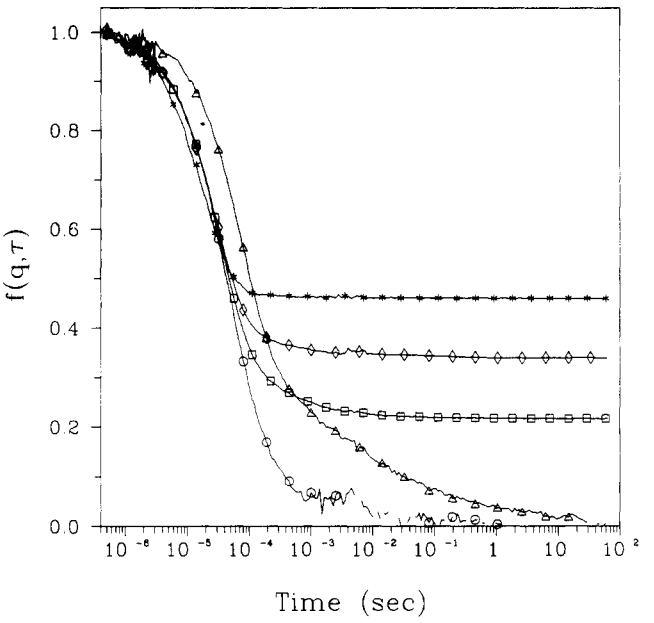

Figure 4. Intermediate scattering functions, $f(q,\tau)$, found from $g_T^{(2)}(q,\tau)$. The data were obtained from a series of samples with C_T ranging from 2% to 10% but with a constant cross-link density $C = 1\%$ at a scattering angle $\theta = 140°$: (○) $C_T = 2\%$, (△) $C_T = 3\%$, (□) $C_T = 4\%$, (◇) $C_T = 5\%$, (*) $C_T = 10\%$.

Also included in Figure 3 is $f_N(q,\tau)$ as obtained from $g_T^{(2)}(q,\tau)$ by using the heterodyne approach,[34] eqs 16 and 18. It is clear that $f_N(q,\tau)$ differs markedly from the other $f(q,\tau)$'s. The steeper initial slope and the absence of a frozen-in component, $f(q,\infty)$, are apparent.

Figure 4 shows intermediate scattering functions for a series of gels with C_T ranging from 2% to 10% but with $C = 1\%$. Macroscopically, a gel becomes stiffer or more rigid when the total monomer content is increased.[1,9] Simultaneously $f(q,\infty)$ is found to increase when the gels are treated as general nonergodic media. At $C_T = 2\%$ and $C_T = 3\%$ with $C = 1\%$ the gels are soft and fluidlike, and as is shown, the corresponding $f(q,\tau)$ decays to a value approaching zero. For larger C_T the $f(q,\infty)$'s become increasingly larger in magnitude, implying that a larger fraction of the density fluctuations becomes frozen-in.

The gelation or rigidity of a gel can also be influenced by the cross-link content.[1,10] As the cross-link content C is increased from 0 to 4% (at $C_T = 2.5\%$), the gel goes from a polymer solution to a rigid solidlike gel. At $C_T = 2.5\%$ the gel threshold or the content of cross-linker necessary to produce a stiff gel is roughly 1.5%.[35] The intermediate scattering functions for a series of gels with varying C from 1 to 4%, but with constant $C_T = 2.5\%$, are shown in Figure 5. From this plot it can be seen that $f(q,\infty)$ approaches zero for the sample with $C = 1.0\%$, but at $C = 1.5\%$ $f(q,\infty)$ becomes nonnegligible and further increases in this quantity are found for the samples with $C = 2.0$, 3.0, and 4.0%.

The measured intermediate scattering functions $f_N(q,\tau)$ (eq 15) were generally found to be nonexponential (see Figure 6). Analyzing the data by the cumulant method,[36] i.e., fitting $\ln [f_N(q,\tau)]$ to $1 - \langle\Gamma\rangle\tau + \mu_2\tau^2/2$. Expressing the nonexponentiality by $Q = \mu_2/\langle\Gamma\rangle^2$, we find at $\theta = 90°$ that $Q \approx 0.4$ for the solutions ($C = 0$, C_T from 2% to 20%) when analyzing data for $f_N(q,\tau)$ such that $f_N(q,\tau) > 0.3$. For gels Q appears to be hardly dependent on cross-link density; e.g., for the samples given in Figure 5, $Q \approx 0.4$. Only for gels at high total monomer concentrations, $C_T = 7\%$ and $C_T = 10\%$, the observed $f_N(q,\tau)$'s were close to single exponentials ($Q \approx 0.04$).

We now compare our results for the functional form of the measured intensity correlation functions with those of others. As shown here and elsewhere,[17] we find reduced initial amplitudes of the time-averaged ICF's (see Figure 2), implying the presence of measurable frozen-in fluctuations in the gel systems. These observations are intriguing especially in view of the ongoing discussion on the discrepancies between the DLS results obtained by different groups in the field. Munch et al.[37] discussed some

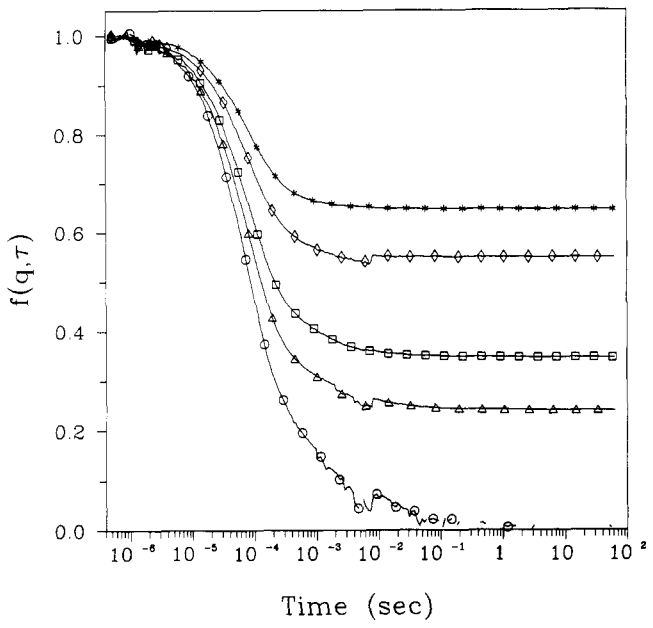

Figure 5. Intermediate scattering functions, $f(q,\tau)$, found from $g_T^{(2)}(q,\tau)$. The data were obtained from a series of samples with C ranging from 1% to 4% but with a constant solid content C_T = 2.5% at a scattering angle θ = 90°: (○) C = 1.0%, (△) C = 1.5%, (□) C = 2.0%, (◇) C = 3.0%, (*) C = 4.0%.

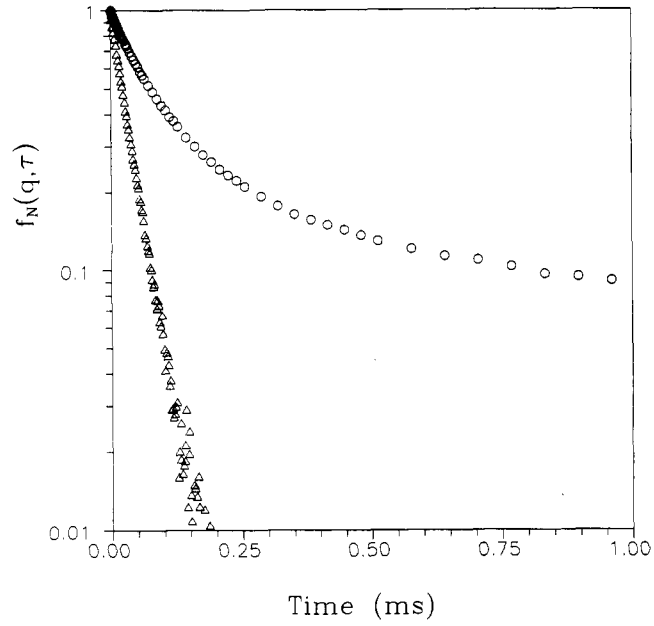

Figure 6. Semilog plot of intermediate scattering functions, $f_N(q,\tau)$, as obtained from $g_T^{(2)}(q,\tau)$ at a scattering angle θ = 90°: (○) C_T = 2.5% and C = 2.0% (normalized second cumulant Q = 0.4), (△) C_T = 10% and C = 2.8% (Q = 0.04).

of the discordant experimental results. These authors find exponential decay curves whereas, e.g., Wun and Carlson[3] have found ICF's that show reduced amplitudes and are clearly nonexponential. The continuum model developed by Tanaka et al.[2] predicts exponential ICF's whereas the model used by Wun and Carlson[3] is based on a harmonically bound Brownian particle and this leads to a nonexponential ICF and yields a reduced initial amplitude of $g_T^{(2)}(q,\tau)$.[17,18] The dispute in the literature also concerns whether DLS experiments on gels have to be interpreted in the homodyne or heterodyne scheme. Some workers in the field,[11,13,38] following the initial work of Tanaka et al.[2] use the homodyne scheme. This, however, is only allowed if the scattered field is a zero-mean Gaussian variable. We have shown, however, while this assumption is valid in the full ensemble, it is not valid for a subensemble (=scattering volume) studied in a single light scattering experiment. Other workers[10,21,37] use the heterodyne detection scheme, and the relation with the nonergodic approach will be dealt with later.

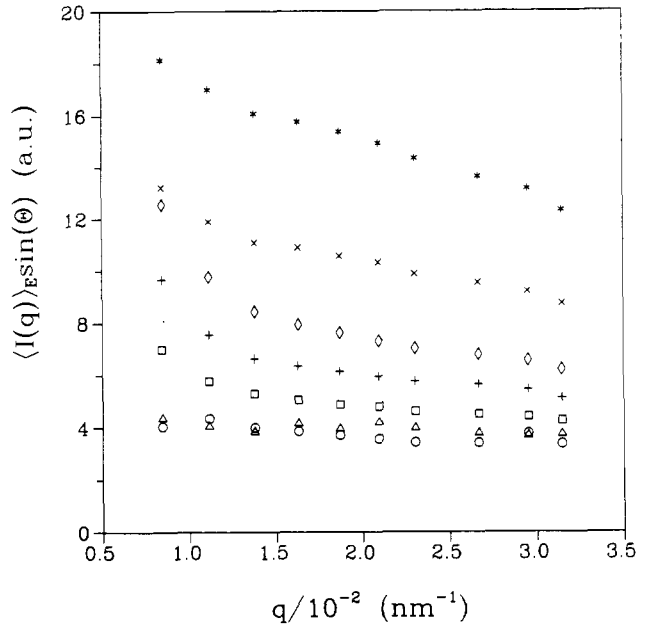

Figure 7. Time-averaged scattered intensities $\langle I(q)\rangle_E \sin(\theta)$ vs scattering vector q. Results for samples with constant total solid content C_T = 2.5% and varying cross-link content: (○) C = 0%, (△) C = 0.5%, (□) C = 1.0%, (+) C = 1.5%, (◇) C = 2.0%, (×) C = 3.0%, (*) C = 4.0%.

Although Fang et al.[13] claim that their PAA gels contain no static heteogeneities, they clearly find a reduced amplitude of the ICF measured on a gel when compared with the ICF found from the corresponding solution. This would imply that they have to take into account the nonergodic nature of their samples and that their homodyne approach is probably questionable. A low initial amplitude of $g_T^{(2)}(q,\tau)$ is also reported in refs 11 and 38, suggesting that the homodyne scheme applied by these authors is liable to the same objections.

Sellen,[8] who clearly recognized some of the problems associated with DLS by nonergodic media, developed a method for determining ensemble-averaged ICF's which involved scanning the detector rather than the sample. Though this method has some problems because of the averaging in q space, an ICF is found that is comparable with $g_E^{(2)}(q,\tau)$ given in Figure 2. This author reports also a shift from nonexponential to single-exponential behavior when the total solids vary from 1.8% to 9%.

Static light scattering: Using the procedure described in section III.B, we obtain $\langle I(q)\rangle_E$ and then apply the sin (θ) correction for varying scattering volumes. For scattering angles ranging from θ = 30° to 150° values of $\langle I(q)\rangle_E \sin(\theta)$ are plotted vs scattering vector q in Figure 7 for samples with C_T = 2.5% and varying cross-link content C from 0 to 4% (the same samples for which the intermediate scattering functions are shown in Figure 5). The first observation is that with increasing C there is an overall increase in the ensemble-averaged intensity. A second observation is an increase in the angular dependence of $\langle I(q)\rangle_E$ sin (θ). At C = 0 and C = 1% the ensemble-averaged intensity is nearly q-independent, but for higher cross-link concentrations the q dependence becomes more pronounced. The latter observation implies the presence of density (concentration) fluctuations having wavelengths on the order of several hundred nanometers.

By using eq 8 we can find the contribution of the fluctuating component, $\langle I_F(q)\rangle_T = \langle I_F(q)\rangle_E$, to $\langle I(q)\rangle_E$. Taking the $f(q,\infty)$ values found from the DLS experiments at different scattering angles for the various samples, we obtain the results depicted in Figure 8. As can be seen from this figure, $\langle I_F(q)\rangle_T \sin(\theta)$ is, within experimental error, q-independent (the sample with C = 1% was omitted from Figure 8 because its state is intermediate between a well-defined solution and a well-defined gel). This result suggests that the dynamic parts of the density fluctuations

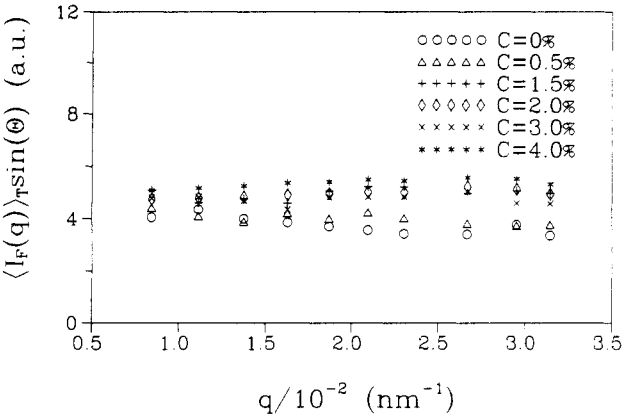

Figure 8. Fluctuating component $\langle I_F(q)\rangle_T \sin(\theta)$ vs scattering vector q for the same set of samples as given in Figure 7. Samples with $C = 0\%$ and $C = 0.5\%$ show ergodic behavior; i.e., $f(q,\infty) = 0$ over the full angular range (θ from 30° to 150°). Sample with $C = 1.0\%$ is omitted because it shows nonergodic behavior for $\theta < 50°$ and ergodic behavior for larger scattering angles.

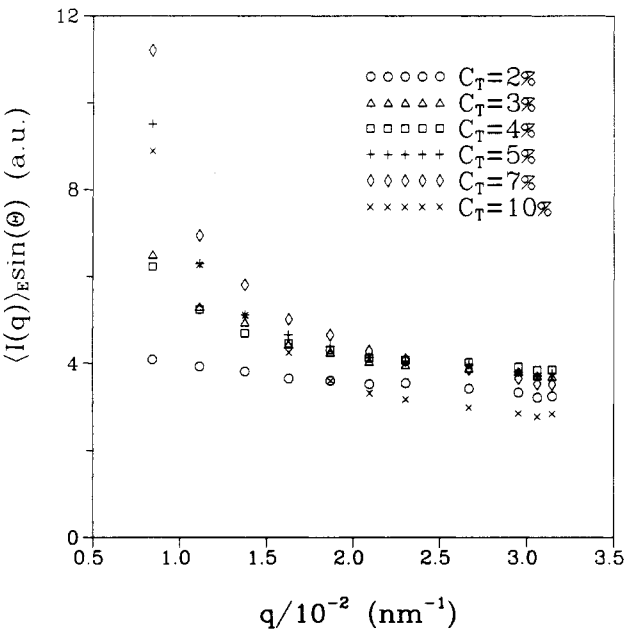

Figure 9. Time-averaged scattered intensities $\langle I(q)\rangle_E \sin(\theta)$ vs scattering vector q for weakly cross-linked gels. Results for samples with constant cross-link density $C = 1\%$ and varying total solid content: (○) $C_T = 2\%$, (△) $C_T = 3\%$, (□) $C_T = 4\%$, (+) $C_T = 5\%$, (◇) $C_T = 7\%$, (×) $C_T = 10\%$.

have a correlation range much smaller than the wavelength of light. Furthermore, the amplitude of these fluctuations appears to increase slightly with increasing cross-link concentration, a finding which conflicts with the intuition that more rigid systems should exhibit reduced fluctuations (see the end of this section for further discussion).

Similar measurements were carried out on a series of weakly cross-linked gels ($C = 1\%$) prepared using different total monomer contents, varying from 2 to 10%. The results for the ensemble-averaged scattered intensities are given in Figure 9 (see Figure 4 for dynamic measurements on the same samples). The "soft gel" with $C_T = 2\%$ shows hardly any q dependence. When C_T is increased above 2%, $\langle I(q)\rangle_E \sin(\theta)$ again becomes q-dependent with relatively large intensities at small scattering vectors. There is a maximum in the low-q intensity at $C_T = 7\%$. All samples suggest a leveling off at high q. In order to compare the angular dependence of the ensemble-averaged scattered intensities of these gels with those of the analogous solutions ($C = 0\%$), we plot the latter in Figure 10. There is again an increase in $\langle I(q)\rangle_E \sin(\theta)$ at low q, and the intensities at large q suggest a decay to a constant value. Actually, it is remarkable that these polymer solutions show this q-dependent scattering because it

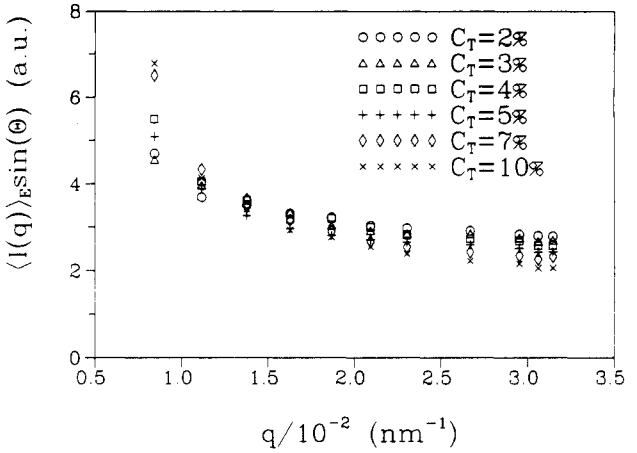

Figure 10. Time-averaged scattered intensities $\langle I(q)\rangle_E \sin(\theta)$ vs scattering vector q for polymer solutions ($C = 0\%$). Variation of total solid content: (○) $C_T = 2\%$, (△) $C_T = 3\%$, (□) $C_T = 4\%$, (+) $C_T = 5\%$, (◇) $C_T = 7\%$, (×) $C_T = 10\%$.

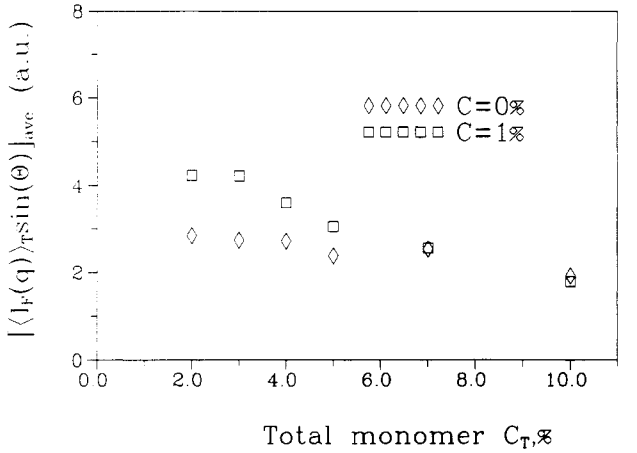

Figure 11. Fluctuating component $[\langle I_F(q)\rangle_T \sin(\theta)]_{ave}$ vs total solid content C_T for the samples given in Figures 9 and 10. Data for $\langle I_F(q)\rangle_T$ are obtained by combining DLS and SLS results, i.e., by using $\langle I_F(q)\rangle_T = \langle I(q)\rangle_E[1 - f(q,\infty)]$ (eq 8) where $f(q,\infty)$ is found from DLS experiments. Results given in the figure are the average over the full angular range of data for $\langle I_F(q)\rangle_T \sin(\theta)$ found at each scattering angle.

is usually thought that typical length scales over which concentration fluctuations occur in these solutions are on the order of ≈5 nm.[14] If these were the only relevant fluctuations, one would expect flat curves in the q regime probed by SLS. The intensities scattered by the cross-linked systems are only slightly larger than those scattered by the equivalent solutions (cf. Figures 9 and 10).

Since the solutions may be regarded as ergodic systems and the cross-linked samples as nonergodic, it is interesting to compare $\langle I_F(q)\rangle_T$ as obtained for the gels with the scattered intensity produced by the corresponding solutions. In Figure 11, the time-averaged fluctuating part, $[\langle I_F(q)\rangle_T \sin(\theta)]_{ave}$, of the total ensemble-averaged intensity is plotted vs monomer concentration C_T. Because the fluctuating components are q-independent (cf. Figure 8), the results given in Figure 11 are the average over the full angular range (θ from 30° to 150°) of data for $\langle I_F(q)\rangle_T \sin(\theta)$ found at each scattering angle. The results suggest that $\langle I_F(q)\rangle_T$ is smaller for the solutions than for the cross-linked samples in the range from $C_T = 2\%$ to $C_T = 5\%$. This observation is similar to the results given in Figure 8. Quantifying the dependence of $\langle I_F(q)\rangle_T$ on C_T by a scaling law, we find $\langle I_F(q)\rangle_T \sim C_T^{-0.21}$ for $C = 0\%$ and $\langle I_F(q)\rangle_T \sim C_T^{-0.55}$ for $C = 1\%$. A number of samples with C_T varying between 2.5% and 10% at constant $C = 2.8\%$ were prepared and measured completely independently from this work.[39] For these samples we found $\langle I_F(q)\rangle_T \sim C_T^{-0.58}$ which agrees, within experimental error, well with the results given in Figure 11 for $C = 1\%$. For polymers in a good solvent one finds,[21] following de Gennes,[14] $\langle I(q)\rangle \sim$

$C_T^{-0.25}$ in the semidilute regime (see eq 24). Apparently the exponent found here for the PAA solutions agrees reasonably well with this value, implying probably that $\langle I_F(q)\rangle_T$ accounts for the density fluctuations described by current theories on static conformations in polymer solutions.[14] Using this reasoning, we conjecture that the larger exponent, found for the concentration dependence of $\langle I_F(q)\rangle_T$ for the gels, reflects poorer solvent conditions for cross-linked systems when compared to un-cross-linked systems.

In comparing our results with those in the literature, we notice that Sellen[8] also found an increase in the scattered intensity at low-q values for polyacrylamide solutions whereas Fang et al.[13] observed q-independent scattering from both PAA solutions and gels. In addition, Sellen[8] observed stationary components in the intensity scattered by un-cross-linked samples at $C_T > 6\%$. We also found similar results for the samples with $C_T = 7\%$ and 10% at angles ≤70°. A possible explanation for these findings is that the finite lifetime, T_r, of the physical entanglements[14,40] is large compared to the duration of an experiment so that the DLS results exhibit effective nonergodic features.

The fluctuating component of light scattered by a semidilute polymer solution or gel can be written[41] as

$$\langle I_F(q)\rangle_E \sim \frac{k_B T C_T^2}{M_{os}} \tag{24}$$

where k_B is Boltzmann's constant, T the temperature, and M_{os} the longitudinal osmotic modulus, which is expected to scale as $C_T^{9/4}$. Our finding, mentioned above, that the gels appear to show slightly larger values of $\langle I_F(q)\rangle_T$ than the equivalent un-cross-linked solutions implies, surprisingly, that the (presumably) more rigid gels have lower moduli than the solutions. A possible explanation of this finding is that some segregation (or "microsyneresis"[14]) may occur on cross-linking, resulting in semimicroscopic regions of high and low polymer concentration whose average modulus is lower than that of the more uniform solution. Such segregation could, of course, also be the source of the large-scale inhomogeneities which give rise to the static component of the scattered intensity.

Diffusion coefficients: To conclude this section, we present the results obtained for the diffusion coefficients of the different systems under study. As pointed out in section I one has the option of treating the DLS data either according to a general nonergodic medium or by using the heterodyne approach. In the following, results for both approaches will be given.

Considering first the gel as a nonergodic medium, we obtain the diffusion coefficient $D(q)$, which describes the average relaxation of all density fluctuations which contribute to the scattering, from the initial decay rate or first cumulant[36] of $f(q,\tau)$ (eq 12). Treating the data according to the heterodyne approach, one finds $D_N(q)$, which describes the relaxation of the dynamic part of the density fluctuations, from the first cumulant of $f_N(q,\tau)$ (eq 19). $D(q)$ can be regarded as resulting from the weighted sum of two "relaxation" processes: one having amplitude $1 - f(q,\infty)$ and diffusion coefficient $D_N(q)$ and the other with amplitude $f(q,\infty)$ and diffusion coefficient zero. This observation becomes apparent if one considers the relation between $f(q,\tau)$ and $f_N(q,\tau)$ which can be found from eqs 1, 2, 5, 7, 8, and 15

$$\begin{aligned} f(q,\tau) &= \langle [E_F(q,0) + E_C(q)][E_F^*(q,\tau) + E_C^*(q)]\rangle_E / \langle I(q)\rangle_E \\ &= [\langle E_F(q,0)\, E_F^*(q,\tau)\rangle_T + \langle I_C(q)\rangle_E] / \langle I(q)\rangle_E \\ &= [1 - f(q,\infty)] f_N(q,\tau) + f(q,\infty) \end{aligned} \tag{25}$$

If the data are incorrectly analyzed as if the medium were ergodic, we obtain, through eq 13, the meaningless apparent diffusion coefficient $D_A(q)$ (related to $D(q)$ by eq 14).

The results for these diffusion coefficients are shown in Figure 12 for a system with $C_T = 2.5\%$ and $C = 4.0\%$. It is clear that there is a distinct difference between $D_A(q)$, $D(q)$, and $D_N(q)$. While $D(q)$ shows a slight dependence on scattering vector q, $D_N(q)$ is essentially independent of q which is at least consistent with the q independence of $\langle I_F(q)\rangle_T$ shown in Figure 8.

We note that given a stiff gel, for which $f(q,\infty)$ approaches 1, the constant component of the intensity I_C is typically greater than the fluctuating component $\langle I_F(q)\rangle_T$. In eq 4 the second term (heterodyne) on the right-hand side is then much greater

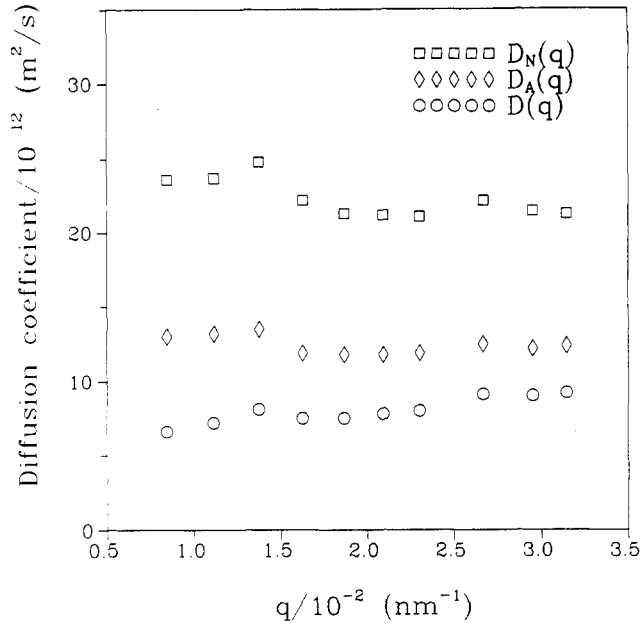

Figure 12. Apparent diffusion coefficient D_A and diffusion coefficients D and D_N against scattering vector q for a system with $C_T = 2.5\%$ and $C = 4.0\%$. D_A is obtained from the initial slope of $[g_T^{(2)}(q,\tau) - 1]^{1/2}$ (eq 13), D is found from the initial slope of $f(q,\tau)$ (eq 12), and D_N is the diffusion coefficient obtained by treating the data according to the heterodyne scheme; i.e., it is the initial slope of $f_N(q,\tau)$ (eq 19).

than the first term. It is straightforward to show, using eqs 13, 15, and 19, that $D_N(q) = 2D_A(q)$ in this limit. The data of Figure 12, for which $f(q,\infty)$ ranges from 0.57 at $\theta = 150°$ to 0.72 at $\theta = 30°$, display roughly this relationship between $D_N(q)$ and $D_A(q)$.

Using only results obtained at $\theta = 90°$, diffusion coefficients of three different sets of samples with varying contents of cross-linker ($C = 0$, 1, and 2.8%) are presented in parts a and b of Figure 13 vs total monomer content. The samples with $C = 2.8\%$ were prepared and measured completely independently from this work.[39] From Figure 13a one notices that $D(q)$ is only weakly dependent on C_T in the concentration range studied for all cross-link ratios C but shows a dependence on C at a fixed C_T. The values for $D_N(q)$, shown in Figure 13b, show an increase with total solids. It is found here and elsewhere[39] that for the cross-linked systems $D_N(q)$ is hardly dependent on the cross-link density. Comparing our results for $D_N(q)$ with those reported in refs 4 and 8, one observes a reasonable agreement. Hecht and Geissler,[4] however, used the pure heterodyne scheme, which means, in our terminology, taking $D_N(q) = 2D_A(q)$. This leads to larger values for $D_N(q)$ when compared to the results obtained by our procedure, i.e., using eq 20 in conjunction with eq 19. The difference is more pronounced for gels at low C_T than for systems at high C_T; e.g., for the sample with $C_T = 4\%$ and $C = 1\%$ $2D_A(q) = 42 \times 10^{-12}$ m^2/s and $D_N = 29 \times 10^{-12}$ m^2/s, whereas for the sample with $C_T = 10\%$ and $C = 1\%$ $2D_A(q) = 74 \times 10^{-12}$ m^2/s and $D_N = 60 \times 10^{-12}$ m^2/s (all data at $\theta = 90°$). Furthermore, $D_A(q)$ appears to be q-dependent (especially at low C_T) whereas $D_N(q)$ is q-independent.

Fitting $D_N(q)$ for the cross-linked samples to a power law shows that $D_N(q) \sim C_T^{0.61}$ for $C = 1\%$ and $D_N(q) \sim C_T^{0.67}$ for $C = 2.8\%$. Within experimental errors we conclude that the exponent is independent of C. These results are compatible with the findings of Hecht and Geissler[4] and Sellen.[8] For the solutions we find $D_N(q) \sim C_T^{0.27}$, which is lower than the exponent measured by Sellen,[8] who found 0.55.

In the viscoelastic model of a polymer network (transient or cross-linked) the diffusion coefficient $D_N(q \to 0)$ is given by[41]

$$D_N = \mu M_{os} \tag{26}$$

where μ is the mobility and M_{os} is the longitudinal osmotic modulus. Thus, combining eqs 24 and 26, we see that the product $\langle I_F(q \to 0)\rangle_E \times D_N(q \to 0)$ is proportional to the mobility. The data of Figures 11 and 13b give $\langle I_F\rangle_E \times D_N \sim 76 C_T^{0.06}$ for the

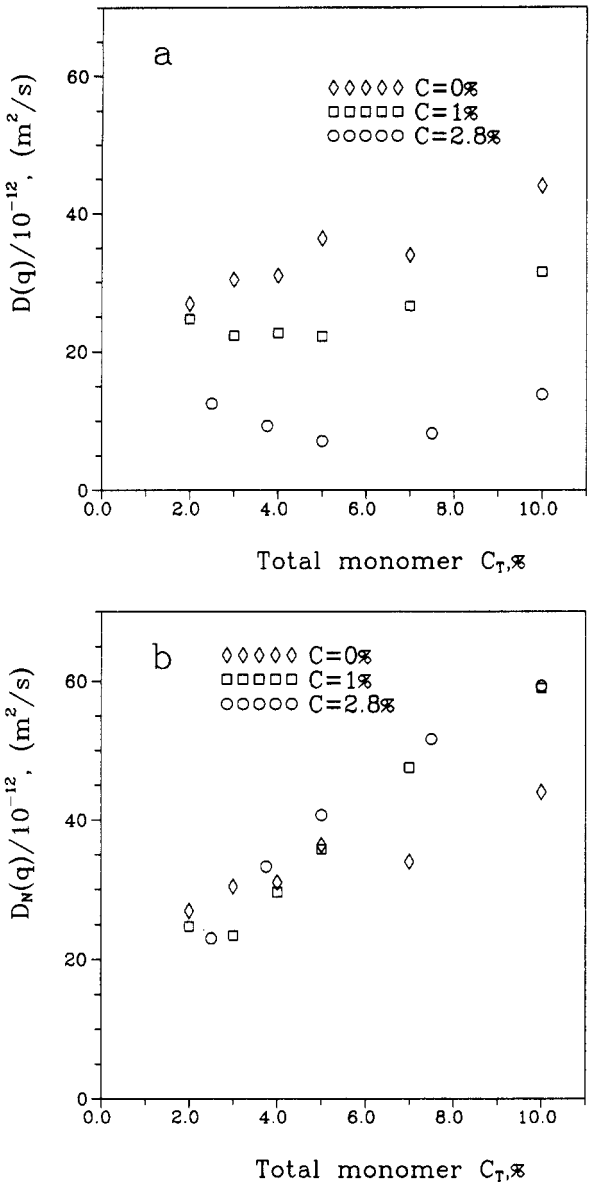

Figure 13. (a) Diffusion coefficient D against total monomer content C_T for polymer solutions (◊, C = 0%) and for cross-linked samples (□, C = 1.0%; ○, C = 2.8%). (b) Diffusion coefficient D_N against total monomer content C_T for the same samples depicted in Figure 13a. The results are obtained at a scattering angle θ = 90°.

solutions (C = 0%) and $\langle I_F\rangle_E \times D_N \sim 98C_T^{0.06}$ for the gels at C = 1%. The error in this exponent is likely to be at least as large as its value so that the apparent, and unexpected, increase of mobility with polymer concentration is probably not real. Nevertheless, the data certainly indicate that the mobility is only a weak function of total polymer concentration in both the solutions and the gels. Furthermore, the mobility in the gels is significantly higher than that in the solutions. As with the osmotic modulus, discussed above, this surprising finding could result from averaging over segregated regions within the gel.

IV. Concluding Remarks

In this paper we have described both static and dynamic light scattering measurements on polyacrylamide gels prepared by polymerization and cross-linking in situ as well as on un-cross-linked solutions. We have pointed out that, in general, gels must be regarded as nonergodic media. As the cross-link density is increased at fixed polymer concentration the measured time-averaged intensity correlation functions show reduced amplitudes $g_T^{(2)}(q,0) - 1$, implying reduced relative intensity fluctuations and the presence of concentration fluctuations within the sample which do not decay completely. Analysis of these intensity correlation functions according to eq 9 provides ensemble-averaged intermediate scattering functions $f(q,\tau$ which describe the evolution in time of all concentration fluctuations in the sample which contribute to the scattering. In turn these intermediate scattering functions may be analyzed to provide quantities such as $D(q)$, the diffusion coefficient describing the average decay of all fluctuations, $f(q,\infty)$, the fraction of the fluctuations which is "frozen-in", and $\langle I(q)\rangle_E[1 - f(q,\infty)]$, the intensity associated with the dynamic (or fully decaying) fraction of the fluctuations.

At this point we could stop and claim to have performed as much analysis as is possible if the samples are regarded simply as arbitrary nonergodic media. Nevertheless, we mention an interesting observation evident from Figures 7 and 8. On increasing the density of cross-links at constant total polymer concentration, the ensemble-averaged scattered intensities increase considerably (Figure 7). However, the dynamic components of the intensity $\langle I_F(q)\rangle = \langle I(q)\rangle_E[1 - f(q,\infty)]$ are much weaker functions of cross-link density and therefore have magnitudes similar to those of the (fully fluctuating) intensity scattered by the solution (no cross-linker, Figure 8). This observation suggests a possible simplifying hypothesis, namely, that the dynamic fluctuations come from the same source (long-wavelength dynamic density fluctuations) in both gels and solutions and that the excess static scattering in gels arises from "uninteresting" large-scale static inhomogeneities. This hypothesis, which has been used (perhaps without full justification) by many earlier workers, allows one to treat the dynamic light scattering in terms of a "heterodyne" mixing between the static light field scattered by the static inhomogeneities and the dynamic field (eq 20).

Support for this point of view comes from the fact that the diffusion coefficient $D_N(q)$, describing the average decay of $f_N(q,\tau)$ (eq 15), the intermediate scattering function associated with the dynamic fluctuations, is essentially independent of the scattering vector (Figure 12). However, this approach also leads us to surprising conclusions. First, we find that the fluctuating components of the intensities scattered by the gels are slightly *larger* than those scattered by the solutions at the same total concentration of polymer (Figures 8 and 11), implying *smaller* osmotic moduli. Second, a combination of static and dynamic light scattering data indicates that the mobility of the polymer in the gel is somewhat *larger* than that in the equivalent solution. We suggested that these surprising findings, as well as the existence of the large-scale inhomogeneities, might result from semimicroscopic segregation in the gels, if the water is a poorer solvent in the presence of cross-links.

We also mention that studies by small-angle neutron scattering show that the intensities scattered by polyacrylamide solutions at relatively low concentrations are essentially independent of q at small q and then decrease for $q > 2\pi/\xi$ where ξ is the spatial correlation length, roughly the spacing between polymer segments.[14] However, for gels at the same concentration, the scattering is much stronger at small q ($q^{-1} \sim 100$ nm), as also observed in the light scattering (Figure 7), and decreases continuously with increasing q, only meeting the curve for the solution at $q \sim 2\pi/\xi$.[7] This suggests that the extra density fluctuations introduced by the cross-linking are present on all spatial scales from >100 nm down to ξ and therefore casts some doubt on the validity of regarding these fluctuations as large-scale and irrelevant. It also seems possible that the magnitude and spatial extent of these

fluctuations may depend on the manner in which the gel is prepared. Thus physical disturbances, such as mechanical vibrations, during the gelling process might have significant effects as might variations in the concentrations of initiator and catalyst in the pregelling mixture. In future work we intend to investigate possible variations of gel structure with conditions of preparation.

Finally we can discuss the expected dynamics of an "ideal" gel, i.e., one not containing extra heterogeneities and showing the same average scattering at all scattering vectors as the solution. As pointed out in section I, such a gel is still nonergodic since, because of the cross-links, it cannot evolve through the complete phase space accessible to the equivalent solution. Therefore, $f(q,\infty)$ cannot be identically zero since some fraction of the density fluctuations cannot decay completely. However, as mentioned above, the results of Figures 8 and 11 show that the fluctuating components of the intensities scattered by gels are actually somewhat larger than those scattered by the equivalent solutions, implying the absence of nonergodic, constant, components if the large-scale inhomogeneities are neglected. Furthermore, Moussaid et al.[42] have recently prepared, from slightly charged (acrylic acid) polymers, gels which do not show an excess scattering. Measured time- and ensemble-averaged intensity correlation functions for these systems are almost identical, again implying the absence of a significant nonergodic component in the scattering. One might speculate that the essentially negligible values of $f(q,\infty)$ found in these systems mean that the polymer segments can typically move locally over distances comparable to the correlation length ξ, so that the time-averaged local density of polymer segments is quite uniform.

It is remarkable that, although gels have been studied for many years by DLS, no theory for the intermediate scattering function $f(q,\tau)$ which takes proper account of the permanent cross-links has been reported. For this reason we have, in this paper, concentrated on the well-defined averaged diffusion coefficients obtained from the initial decays of the intermediate scattering functions rather than on their detailed functional forms.

Acknowledgment. We gratefully acknowledge the fruitful discussions with Dr. S. J. Candau and Dr. J. Bastide regarding properties of gels. Dr. E. Geladé is thanked for his help in the experiments.

References and Notes

(1) Baselga, J.; Hernández-Fuentes, I.; Piérola, I. F.; Llorente, M. A. *Macromolecules* **1987**, *20*, 3060.
(2) Tanaka, T.; Hocker, L. O.; Benedek, G. B. *J. Chem. Phys.* **1973**, *59*, 5151.
(3) Wun, K. L.; Carlson, F. D. *Macromolecules* **1975**, *8*, 190.
(4) Hecht, A. M.; Geissler, E. *J. Phys. (Les Ulis, Fr.)* **1978**, *39*, 631.
(5) Geissler, E.; Hecht, A. M. *J. Phys. (Les Ulis, Fr.)* **1978**, *39*, 955.
(6) Geissler, E.; Hecht, A. M.; Duplessix, R. *J. Polym. Sci., Polym. Phys. Ed.* **1982**, *20*, 225.
(7) Hecht, A. M.; Duplessix, R.; Geissler, E. *Macromolecules* **1985**, *18*, 2167.
(8) Sellen, D. B. *J. Polym. Sci., Polym. Phys. Ed.* **1987**, *25*, 699.
(9) Geissler, E.; Hecht, A. M.; Horkay, F.; Zrinyi, M. *Macromolecules* **1988**, *21*, 2594.
(10) Mallam, S.; Horkay, F.; Hecht, A. M.; Geissler, E. *Macromolecules* **1989**, *22*, 3356.
(11) Takebe, T.; Nawa, K.; Suehiro, S.; Hashimoto, T. *J. J. Chem. Phys.* **1989**, *91*, 4360.
(12) Peters, A.; Schosseler, F.; Candau, S. J. In *Polymers in Aqueous Media*; Glass, J. E., Ed.; Advances in Chemistry Series; American Chemical Society: Washington, DC, 1989; p 45.
(13) Fang, L.; Brown, W.; Konak, C. *Polymer* **1990**, *31*, 1960.
(14) de Gennes, P.-G. *Scaling Concepts in Polymer Physics*; Cornell University Press: Ithaca, NY, 1979.
(15) Pusey, P. N.; van Megen, W. *Phys. Rev. Lett.* **1987**, *59*, 2083.
(16) Pusey, P. N.; van Megen, W. *Ber. Bunsen-Ges. Phys. Chem.* **1990**, *94*, 225.
(17) Joosten, J. G. H.; Geladé, E. T. F.; Pusey, P. N. *Phys. Rev. A* **1990**, *42*, 2161.
(18) Pusey, P. N.; van Megen, W. *Physica A* **1989**, *157*, 705. This paper contains a detailed discussion of our use of the term "nonergodic", a usage which, though common in the literature on glasses, still appears to engender controversy.
(19) Dusek, K.; Prins, W. *Adv. Polym. Sci.* **1969**, *6*, 1.
(20) Bastide, J.; Leibler, L. *Macromolecules* **1988**, *21*, 2647.
(21) Candau, S. J.; Young, C. Y.; Tanaka, T.; Lemarechal, P.; Bastide, J. *J. Chem. Phys.* **1979**, *70*, 4694.
(22) Jakeman, E. In *Photon Correlation and Light Beating Spectroscopy*; Cummins, H. Z., Pike, E. R., Eds.; Plenum Press: New York, 1974; p 75.
(23) Geissler, E.; Hecht, A. M. *J. Chem. Phys.* **1976**, *65*, 103.
(24) Actually, eq 16 is a solution of the quadratic (eq 20) for $f_N(q,\tau)$.
(25) Stein, R. S.; Soni, V. K.; Yang, H.; Erman, B. In *Biological and Synthetic Networks*; Kramer, O., Ed.; Elsevier Applied Science: Amsterdam, The Netherlands, 1988; and references therein.
(26) Wun, K. L.; Prins, W. *J. Polym. Sci., Polym. Phys. Ed.* **1974**, *12*, 533.
(27) Weiss, N.; van Vliet, T.; Silberberg, A. *J. Polym. Sci., Polym. Phys. Ed.* **1981**, *19*, 1505.
(28) Schätzel, K.; Drewel, M.; Stimac, S. *J. Mod. Opt.* **1988**, *35*, 711.
(29) In writing eq 4 we have neglected complications due to spatial averaging and mixing efficiency.[30] In practice, the first term on the right-hand side of eq 4 (homodyne term) must be multiplied by β^2 ($\langle 1$) expressing partial spatial coherence effects whereas the second term in eq 4 (heterodyne term) must be multiplied by α ($\langle 1$) expressing incomplete mixing efficiency. Effects of spatial integration for DLS on nonergodic media have been discussed in ref 18. In general, $\alpha \neq \beta$, but here we take $\alpha = \beta$ which is rationalized by the fact that we use a detector system such that β is close to 1. Then solving eq 4 with these modifications for the nonergodic case gives (cf. eq 9) $f(q,\tau) = 1 + [\{g_T^{(2)}(q,\tau) - 1 - \sigma_I^2)/\beta^2 + 1\}^{1/2} - 1]/Y$. For the heterodyne treatment, similar modifications have to be made to eq 16.
(30) Cummins, H. Z.; Swinney, H. L. In *Progress in Optics VIII*; Wolf, E., Ed.; North-Holland: Amsterdam, The Netherlands, 1970; p 133.
(31) Mackie, W.; Sellen, D. B.; Sutcliffe, J. *Polymer* **1978**, *19*, 9.
(32) Kobayasi, S. *Rev. Sci. Instrum.* **1985**, *56*, 160.
(33) It is easy to show that, by using eq 9, the final $f(q,\tau)$ depends sensitively on β, especially for values of $\sigma_I^2/\beta^2 > 0.6$; e.g., for the data given in Figure 3, we find that taking $\beta = 0.92$ gives $f(q,\infty) = 0.40$ instead of $f(q,\infty) = 0.45$ when $\beta = 0.945$ (which is the value used in Figure 3).
(34) Apparently, it has not been realized before that the quadratic (eq 20) can be solved for $f_N(q,\tau)$ (see eq 16). In conjuction with eq 18 this yields also the intensity of the concentration fluctuations as, e.g., discussed by Geissler et al.[9] without making any assumptions of a full heterodyne or complete homodyne detection mode. It should be noted, however, that using this method also requires a well-defined optical detection system, i.e., $\beta \approx 1$.
(35) Bansil, R.; Gupta, M. K. *Ferroelectrics* **1980**, *30*, 63.
(36) Koppel, D. E. *J. Chem. Phys.* **1972**, *57*, 4814.
(37) Munch, J. P.; Candau, S.; Hild, G. *J. Polym. Sci., Polym. Phys. Ed.* **1977**, *15*, 11.
(38) Oikawa, H.; Murakami, K. *Macromolecules* **1991**, *24*, 1117.
(39) Joosten, J. G. H.; Geladé, E. T. F., unpublished results.
(40) de Gennes, P.-G. *Macromolecules* **1976**, *9*, 587.
(41) Candau, S. J.; Bastide, J.; Delsanti, M. *Adv. Polym. Sci.* **1982**, *44*, 27.
(42) Moussaid, A.; Munch, J. P.; Schosseler, F.; Candau, S. J. *J. Phys. II (Les Ulis, Fr.)* **1991**, *1*, 637.

Registry No. AA (homopolymer), 25034-58-6; (AA)(BAA) (copolymer), 9003-05-8.